

# Flaw of photonic band structure and misunderstanding of photonic bound state in the continuum

Shahin Firuzi

*Department of Precision Instrument, Tsinghua University, 100084 Beijing, People's Republic of China*

We show an important flaw in the photonic band structure which forms the basis of our understanding of crystal momentum in photonic systems. We investigate the origin of this flaw and propose a continuous band structure as the rectification. Based on the proposed continuous photonic band structure, a bound state in the continuum (BIC) is actually below the light line, similar to the conventional guided modes. We present the condition for the boundedness of photonic modes and confirm the effectiveness of our condition via two photonic crystal slabs with resonance-trapped BIC and symmetry-protected BIC, respectively. In the second case, our condition of boundedness correctly indicates a radiative mode, which satisfies the condition of symmetry-protected BIC based on the conventional folded band structure.

The concept of photonic band structure was first introduced by Eli Yablonovitch [1] and Sajeev John [2] in 1987, showing that a photonic band gap similar to electronic band gap can be generated in periodic photonic structures, in which all the electromagnetic fields are suppressed. The theoretical basis and methodology of deriving the photonic band structure were developed later in 1990 [3], which became the basis for the future designs. Photonic crystals and metamaterials, whose building blocks have different optical sizes [4], both utilize the photonic band structures to realize novel photonic phenomena such as zero index of refraction [5–8] and bound state in the continuum (BIC) [9–12].

According to the current understanding of BICs in photonic community [12], BIC modes, unlike guided modes, are located above the light line of the surrounding materials but are still confined within the photonic crystal slab. In this letter, we show that the concept of photonic band structure has a fundamental flaw in its derivation methodology [3], leading to misunderstanding of the photonic band structure, especially concepts regarding the position of the modes relative to the light line. One misunderstanding is that the BIC modes are located above the light line. By correcting the fundamental flaw of photonic band structure, we show that BIC modes are actually located below the light line, and are induced by the total internal reflection, similar to the guided modes. We propose two conditions for any bounded mode through which we describe the behavior of BIC modes.

To show the connection between BIC modes and guided modes, we try to understand the boundedness due to the total internal reflection in an intuitive manner. We show that guided modes due to total internal reflection can be described, similar to BIC modes, by the destructive interference of the field at the boundary of two materials. We consider a two-dimensional model of a boundary between two materials: light propagates from the lower medium (material 1) with the refractive index  $n_1$  (in this example, silicon) to the upper medium (material 2) with index  $n_2$  (vacuum) with an incident angle  $\theta_i$  (Fig. 1). In the case of  $\theta_i$

is larger than the critical angle  $\theta_c = \sin^{-1}(n_2/n_1)$ , total internal reflection happens so the light reflects back to the silicon slab from the boundary. The wave above the boundary is an evanescent wave. Such a wave's field distribution along the boundary consists of many pairs of fields with opposite phases (red and blue spots in Fig. 1a). For each of these pairs, the two fields interfere with each other destructively, leading to the cancellation of fields in the farfield.

The wavevector of the wave inside material 1 has a magnitude of  $k_1 = n_1 \omega/c$ , which can be decomposed to its components along  $x$  and  $y$  axes, given as  $k_1^x = k_1 \sin \theta_i$  and  $k_1^y = k_1 \cos \theta_i$ , respectively. Under the condition of total internal reflection, along the boundary between the slab and vacuum, the total  $y$  components of the incident and reflected wavevectors becomes zero, and the wave propagates along  $x$  with the wavevector  $k_1^x = k_1 \sin \theta_i$ . According to  $k_1^x$ , we can define the corresponding wavelength for the wave along the boundary as  $\lambda_b = 2\pi/k_1^x$ , which is the same on both sides of the boundary. By defining  $\lambda_b$  and the wavelength of the light in material 2 (vacuum) as  $\lambda_2$ , we can write  $\lambda_b = \lambda_2/\sin \theta_0$ . This can be used to achieve the condition of boundedness due to the total internal reflection: when  $\lambda_b < \lambda_2$ , there is no real  $\theta_0$  satisfying  $\lambda_b = \lambda_2/\sin \theta_0$ , leading to the total internal reflection (Fig. 1a). However, for  $\lambda_b \geq \lambda_2$ , we can find a propagation angle  $\theta_0$  in material 2 to satisfy  $\lambda_b = \lambda_2/\sin \theta_0$ , leading to the wave propagating in material 2 (Fig. 1b).

From Fig. 1 it is clear that for a wave with  $\lambda_b \geq \lambda_2$ , it always leaks to medium 2. We can interpret the condition  $\lambda_b < \lambda_2$  in the wavevector space as  $k_1^x > k_2$ . I.e. for a given frequency, if we want to bound the light inside material 1, the momentum along the boundary has to be larger than that of the surrounding material — the mode is below the light line in the band structure.

We need to consider the fact that at a flat boundary between two homogenous bulk materials, the neighboring field profiles with opposite phases are identical in amplitude

and shape along the boundary, giving the possibility of complete destructive interference with each other in the farfield. However, the only condition preventing them from a complete cancellation is  $k_1^x \leq k_2$ , which means the mode is located above the light line of material 2. Therefore, even for a mode with identical profile of neighboring fields (which is the case of symmetry-protected BICs [13]), the mode has to be below the light line to be bounded, which is clearly contradictory to our current understanding of BIC modes [12, 13].

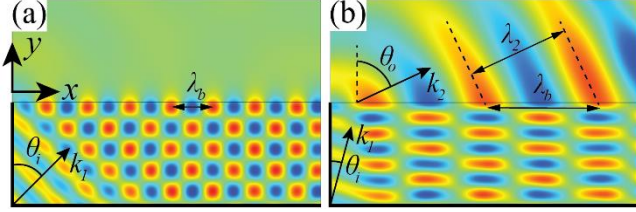


FIG. 1. Light incident from a silicon slab (bottom, material 1) to the vacuum (top, material 2) with an incident angle of (a)  $\theta_i = 45^\circ$  and (b)  $\theta_i = 15^\circ$ .

Here, we discuss the source of the contradictions regarding the concept of light line in photonic band structures, leading to several misunderstandings including BIC modes. To understand the source of this problem, we refer to the original methodology of deriving the photonic band structures [3], in which the authors adopted the standard Bloch theorem from the electronic band structures to the photonic band structures. For an electron in a Bloch state we have

$$\psi = e^{ik \cdot r} u \quad (1)$$

where  $\psi$  is the wave function,  $u$  is a periodic function with the periodicity of the potential,  $r$  is position, and  $k$  is the crystal momentum vector. For the state of electrons in crystalline solids, the crystal momentum is restricted within the reciprocal lattice vector  $K$ , implying that the momentum of an electron in a discrete lattice is given as  $k+mK$  for any arbitrary  $m$  where  $m \in \mathbb{Z}$ . This is resulted from the discrete nature of the crystalline solids, which consist of a set of discrete atoms. Electrons oscillate around each of these atoms, forming an electronic wave in the crystal. Therefore, the electronic wave can be considered as a set of discrete oscillating points. In such a system, there are infinite number of discrete wavelengths (momentums) which can fit the phase distribution of those discrete points, governed by the spatial Nyquist frequency which corresponds to the (shortest wavelength) largest momentum supported by the structure,  $K$ . We can describe this concept in an intuitive way as follows. By increasing the energy of the electrons, the crystal momentum increases until it reaches the value of the reciprocal lattice vector  $K$ . Beyond  $K$ , as the energy continues to increase, the crystal momentum decreases until it becomes zero again. Such a cycle repeats as the energy

continues to increase. This is the basis of the electronic band structure, in which the energy-momentum relationship can be described completely in the first Brillouin zone by applying the folded bands to each mode. As a result, each crystal momentum corresponds to an infinite number of discrete energies. In this case, the folded nature of the bands is the true representation of the band structure which is a direct result of the discreteness of the system.

Unlike the discrete electronic periodic structures, photonic structures such as the photonic crystals are continuous, in which the photons can exist at any point of the structure. Therefore, a finite spatial Nyquist frequency doesn't exist. Hence, the wavevector (momentum) of the photons increases continuously as their frequency (energy) increases. In such a system, a unique wavevector can be assigned to a mode at any frequency, resulting in a continuous band structure. Hence, applying a folded band structure to photonic systems is improper. In such a continuous band structure, the position of the modes relative to the light line of the surrounding material is essentially different from that of a folded band structure. This flaw of the photonic band structure leads to some misconceptions based on the position of the modes in the band structure, such as the BIC modes determined by the position of high quality-factor modes relative to the light line. We show the difference between folded and continuous band structures via a classic design which was used to experimentally demonstrate the trapped light within the radiation continuum for the first time [11].

The original band structure in [11] is shown in Fig. 2(b). Here, for simplicity we only plot the band structure from  $\Gamma$  ( $k_x=0, k_y=0$ ) to X ( $k_x=0.5, k_y=0$ ). It can be seen that high quality-factor TM-like mode near  $k_x=0.27$  is classified as a resonance-trapped BIC [11]. Based on the conventional folded band structure in Fig. 2(b), this high quality-factor mode is above the light line of glass (surrounding material) hence should be identified as BIC mode. However, the continuous band structure of the same structure (Fig. 2a) clearly shows that the high quality-factor mode is below the light line of glass and should be classified as a guided mode.

In order to clarify the underlying physics of boundedness, we introduce two conditions for a bounded mode. A mode needs to satisfy following two conditions to be bounded in a photonic structure:

1. The mode is below the light line of the surrounding material in the continuous band structure.
2. Over the boundary of a photonic structure, for each field component contributing to the radiation, the absolute value of the sum of negative field should be equal to that of the positive field (i.e. possibility of total destructive interference).

The first condition is the direct result of the fact that the photonic structures are not discrete. Here, we expand the second condition to get a better understanding of the interference of a high quality-factor mode. For a photonic structure radiating in a certain direction, only the field

components perpendicular to the radiation direction contribute to the radiation. E.g. to study the radiation along  $z$  direction, we only need to consider  $E_x, E_y, H_x$  and  $H_y$ . Furthermore, some of these field components may be absent according to the polarization of light (eg. TE or TM). To study the BIC behavior of a system with a radiation channel in  $z$  direction, we consider the equation for the equality of each field corresponding to this radiation channel as

$$Q_F^z = \left| \int_{y_0}^{y_\infty} \int_{x_0}^{x_\infty} F dx dy \right| \quad (2)$$

where  $F$  is the complex field component,  $x_0$  and  $x_\infty$  as well as  $y_0$  and  $y_\infty$  are the lower and upper boundaries of the integration area along  $x$  and  $y$  axes, respectively. By replacing  $F$  with a particular field component such as  $H_x$ , we can derive the equality of that field component along  $z$  direction, such as  $Q_{H_x}^z$ . Although we only consider  $z$  direction here, Eq. (2) can be applied to any direction and its corresponding field components. Because the result of the double integral in Eq. (2) is a complex number, Eq. (2) calculates its absolute value via  $|\cdot|$ . For bounded modes, Eq. (2) gives a value approaching zero, implying a total destructive interference in the farfield. The boundaries of the integration should be defined in a way to cover complete spatial wavelengths of the mode along  $x$  and  $y$  directions ( $\lambda_x = 2\pi/k_x$  and  $\lambda_y = 2\pi/k_y$ ), resulting in  $x_\infty - x_0 = \lambda_x$  and  $y_\infty - y_0 = \lambda_y$ . If the wavevector along any of these directions, such as  $x$ , is zero (uniform spatial phase along that direction), the integration along that specific direction only needs to cover one period of the structure along that specific direction such as  $x_\infty - x_0 = a$  where  $a$  is the periodicity along  $x$ .

To confirm our conditions of boundedness in terms of Eq. (2), we calculate the equalities of the example in Fig. 2. For the TM-like mode, we calculate the equalities of  $H_x$  and  $H_y$  for radiation in  $z$  direction. As shown in Fig. 2(c),  $Q_{H_x}^z$  is small for all the values of  $k_x$  while  $Q_{H_y}^z$  shows valleys at  $k_x = 0.5, 0.73, 1$ , leading to the conclusion that modes at  $k_x = 0.5, 0.73, 1$  satisfy our second condition of boundedness. And, considering that all modes in Fig. 1(a) satisfy first condition of boundedness, the modes at  $k_x = 0.5, 0.73, 1$  should be bounded modes according to our conditions of boundedness, matching the computed quality factors shown in Fig. 2(a) perfectly.

Here, we would like to show the significance of our first condition of boundedness for the existence of bounded modes. We apply our boundedness conditions to a case of symmetry-protected BIC (Fig. 3), in which our second condition is satisfied at  $k_x = 0, 0.5, 1$  due to the anti-symmetric nature of the field. Because the existence of symmetry-protected BIC doesn't depend on the geometrical parameters of the structure as long as the mirror symmetry of the structure is maintained [13], we are able to manipulate the design parameters without breaking the second condition of boundedness. In this design example, a 2D periodic

structure with a periodicity of  $a = 1073$  nm and a thickness of  $h = 340$  nm is considered (Fig. 3a). We consider two designs with different stripe widths of  $w = 142$  nm (slim design, Fig. 3b) and  $w = 222$  nm (wide design, Fig. 3c). The structure only has two loss channels via the out-of-plane radiations upward to the air and downward to the substrate. The structure is excited by a TE-polarized light at a wavelength of 1550 nm.

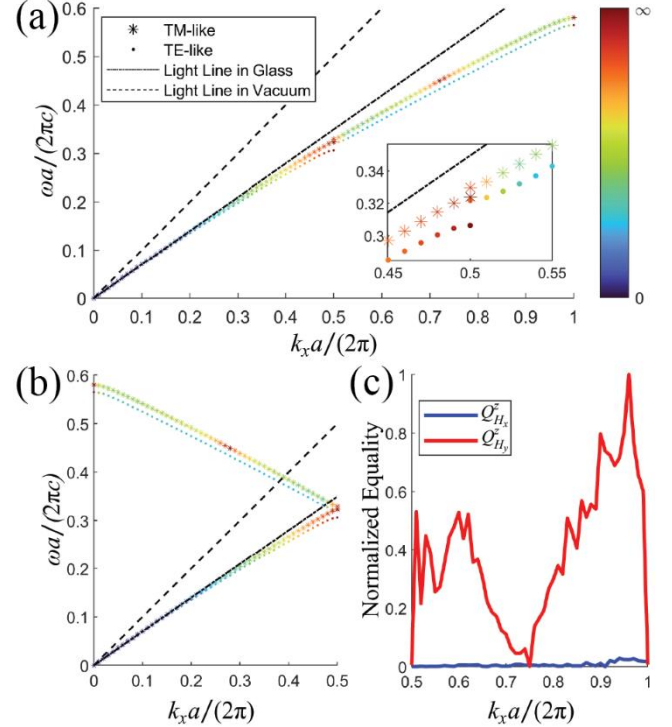


FIG. 2. (a) Continuous (the inset shows the magnified region from  $k_x = 0.45$  to  $0.55$ ) and (b) folded band structures as well as (c) the equality of magnetic field components at the boundary of a photonic crystal slab [11]. In (a) and (b), colormap shows the quality factor of modes.

According to the conventional photonic band structure, the symmetry-protected BIC mode 2 at  $k_x = 0$  (corresponding to mode 2 at  $k_x = 1$  in the continuous band structure Fig. 3d, e) for both designs are above the light lines of both glass and vacuum. However, in the continuous band structure, the locations of the symmetry-protected mode 2 relative to the glass's light line are different for slim and wide stripe designs. In the slim design, mode 2 is located right above the light line of the glass (inset of Fig. 3d). However, this mode of the wide design is below the glass' light line near  $k_x = 1$  (Fig. 3e). For the slim design, mode 2 is always above the light line of continuous band structure despite its symmetry-protected mode profile at  $k_x = 1$  ( $k_x = 0$  in the conventional band structure), hence it is not bounded and show low quality factor from  $k_x = 0$  to  $k_x = 1$  (Fig. 3f). However, in Fig. 3(g), mode-2's quality factor of the wide design increases by a factor of  $10^7$  exactly at the point where the mode goes below the light line of glass.

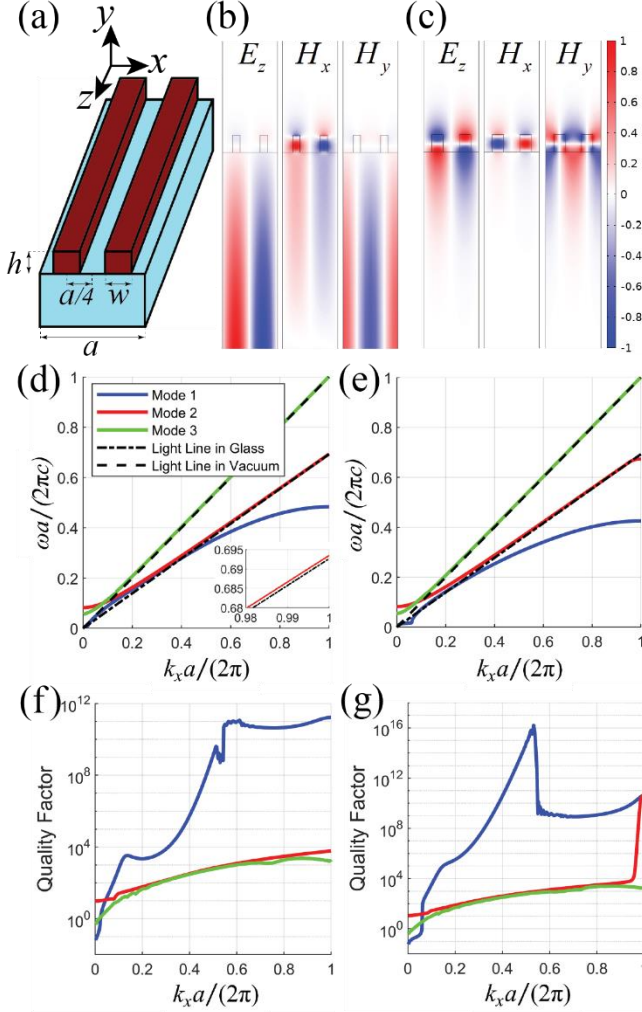


FIG. 3. Structure, field profiles, band structures and quality factors of a 2D photonic crystal. (a) Schematic of the 2D photonic crystal made of silicon stripes on silica substrate. The field profiles of mode 2 of (b) slim and (c) wide designs at  $k_x=1$ . The continuous band structures of the (d) slim (the inset shows the magnified region near  $k_x$  approaching 1) and (e) wide designs. The quality factor of mode 2 (red line) of the (f) slim and (g) wide designs.

The conventional viewpoint of BICs cannot explain the low quality-factor of a symmetry-protected mode at the highly symmetrical point  $k_x=1$  (Fig. 3d, f). However,

according to our conditions of boundedness, it is clear that for the slim design, the quality factor stays low because the mode is above the light line. For the wide design, the high quality-factor near  $k_x=1$  is caused by the fact that mode 2 goes below the light line (Fig. 3e, g). This example demonstrates that the continuous band structure gives the correct interpretation of the boundedness of modes.

Here, we present a clear understanding of the photonic BIC modes. In the case of a symmetry-protected BIC, our second condition of boundedness is satisfied at  $k_x=0, 0.5, 1$ . However, the first condition is only satisfied at  $k_x$  where the mode goes below the light line due to the quadratic dispersion of the dispersion curve. For the resonance-trapped BICs, however, the mode is below the light line for a large portion of the dispersion curve, satisfying the first condition of boundedness. In this case, BIC occurs when the second condition is satisfied at some specific points (wavevectors) of the band structure, where the first condition of boundedness is already satisfied.

This work reveals a fundamental flaw of photonic band structures. This flaw originates from the adoption of folded band structure from electronic crystals to photonic crystals without considering an essential difference between electronic and photonic crystals — electronic crystal is discrete while its photonic counterpart is continuous. We proposed that continuous systems such as photonic crystals should be characterized by the continuous band structures. We showed that in the continuous band structures, all the bounded modes are below the light lines of the surrounding media. We presented two conditions for determining the boundedness of photonic modes. Our conditions successfully confirmed the existence of a resonance-trapped BIC mode. By using the proposed continuous band structure, a symmetry-protected BIC was studied. Due to the intrinsic mode symmetry of symmetry-protected BIC modes, they always satisfy our second condition of boundedness. We showed that for a design in which the mode is above the light line, the quality factor is always low. However, by changing a structural parameter, the mode can go below the light line at certain wavenumbers in the continuous band structure, leading to a dramatic increase in the quality factor.

The author would like to thank Yang Li, Yuanmu Yang, Tian Dong, and Zheng Zhang for discussions.

[1] E. Yablonovitch, Phys. Rev. Lett. 58, 2059 (1987).  
[2] S. John, Phys. Rev. Lett. 58, 2486 (1987).  
[3] S. Satpathy, Ze Zhang, and M. R. Salehpour, Phys. Rev. Lett. 64, 1239 (1990).  
[4] M. V. Rybin, D. S. Filonov, K. B. Samusev, P. A. Belov, Y. S. Kivshar, M. F. Limonov, Nat. Commun. 6, 10102 (2015).  
[5] X. Q. Huang, Y. Lai, Z. H. Hang, H. H. Zheng, and C. T. Chan, Nat. Mater. 10, 582-586 (2011).

[6] P. Moitra, Y. M. Yang, Z. Anderson, I. I. Kravchenko, D. P. Briggs, and J. Valentine, Nat. Photonics 7, 791-795 (2013).  
[7] Y. Li, S. Kita, P. Muñoz, O. Reshef, D. I. Vulis, M. Yin, M. Lončar, E. Mazur, Nat. Photonics 9, 738-742 (2015).  
[8] N. Kinsey, C. DeVault, A. Boltasseva, V. M. Shalaev, Nat. Rev. Mater. 4, 742-760 (2019).  
[9] D. C. Marinica, A. G. Borisov, S. V. Shabanov, Phys. Rev. Lett. 100, 183902 (2008).

- [10] Y. Plotnik, O. Peleg, F. Dreisow, M. Heinrich, S. Nolte, A. Szameit, M. Segev, *Phys. Rev. Lett.* 107, 183901 (2011).
- [11] C. W. Hsu, B. Zhen, J. Lee, S.-L. Chua, S. G. Johnson, J. D. Joannopoulos, M. Soljačić, *Nature* 499, 188–191 (2013).
- [12] C. W. Hsu, B. Zhen, A. D. Stone, J. D. Joannopoulos, M. Soljačić, *Nat. Rev. Mater.* 1, 1–13 (2016).
- [13] A. I. Ovcharenko, C. Blanchard, J.-P. Hugonin, C. Sauvan, *Phys. Rev. B* 101, 155303 (2020).